# Late Cenozoic landscape evolution on lava flow surfaces of the Cima volcanic field, Mojave Desert, California

STEPHEN G. WELLS *Department of Geology, University of New Mexico, Albuquerque, New Mexico 87131*
JOHN C. DOHRENWEND *U.S. Geological Survey, 345 Middlefield Road, MS-941, Menlo Park, California 94025*
LESLIE D. McFADDEN *Department of Geology, University of New Mexico, Albuquerque, New Mexico 87131*
BRENT D. TURRIN *U.S. Geological Survey, 345 Middlefield Road, MS-941, Menlo Park, California 94025*
KENNETH D. MAHRER *Teledyne Geotech, 3401 Shiloh Avenue, Garland, Texas 75043*

## ABSTRACT

**Landscape evolution in the eastern Mojave Desert is recorded by systematic changes in Pliocene to latest Pleistocene volcanic landforms that show discrete periods of eolian deposition, surface stabilization, drainage-network expansion, and erosion on basaltic lava flows. These processes are documented by K-Ar dating in conjunction with morphometric, sedimentologic, pedologic, and geophysical studies. Lava-flow surfaces are composed of constructional bedrock highs and accretionary eolian mantles with overlying stone pavements. The stratigraphy of these mantles records episodic, climatically induced influxes of eolian fines derived from playa floors and distal piedmont regions. The relative proportions of mantle and exposed bedrock vary with flow age, and flows between 0.25 and 0.75 m.y. old support the most extensive eolian mantle and pavement reflecting landscape stability. Drainage networks evolve on flows by (1) rapid initial extension, (2) maximum extension and elaboration, and (3) abstraction of drainage. Increases in bedrock exposures and erosion of the eolian mantle on flows >0.70 m.y. old coincide with maximum drainage extension and significant changes in soil and hydrologic properties within this mantle. Increasing the content of pedogenic clay and $CaCO_3$ causes the accretionary mantle's permeability to decrease; decreased mantle permeability promotes increased runoff, surface erosion, and drainage development. In the late Cenozoic landscape evolution of lava flows, four major stages reflect variations in landscape stability that are controlled by the impact of episodic influxes of eolian fines and increasing soil-profile development on infiltration-runoff properties of the flow surfaces.**

## INTRODUCTION

The morphology of volcanic landforms is used as a basis for the classification of volcanic activity (Rittmann, 1962; Ritter, 1978) and for interpretations of the styles and rates of volcanic eruptions (Wood, 1980). Few studies, however, use volcanic landforms to interpret types, rates, and magnitudes of the surficial processes that modify volcanic forms. Basaltic lava flows form rapidly, are datable by K-Ar analysis, and have original constructional surfaces. Rates at which long-term surficial processes modify these volcanic landforms can thus be measured by analyzing several lava flows of similar origin and composition but of significantly different ages and by comparing surface morphologic differences between flows of different ages.

The late Cenozoic Cima volcanic field in the eastern Mojave Desert of California provides an excellent setting for studying long-term landscape evolution. This field contains K-Ar–dated basalt flows that range in age from late Miocene to latest Pleistocene (Dohrenwend and others, 1984a; Turrin and others, 1984) and that are mainly spatially separated and do not overlap (Fig. 1). The flows were erupted into an environment of long-term erosion (Dohrenwend and others, 1984b); therefore, many flow surfaces have remained subaerially exposed since eruption. The flow surfaces have developed accretionary mantles of coarse deposits composed of weathered and colluviated bedrock (here referred to as "rubble") and fine deposits of eolian origin trapped by the irregular flow surfaces (Fig. 2A).

The primary purposes of this paper are to (1) specify the properties of bedrock constructional forms, drainage networks, and accretionary mantles developed on lava-flow surfaces in the Cima volcanic field, (2) elucidate long-term surficial processes that have shaped these flow surfaces, and (3) develop an evolutionary sequence for the landscapes on late Cenozoic basaltic lava flows in the Mojave Desert.

## METHODOLOGY

Detailed morphologic transects on ten K-Ar–dated flows have been combined with photogeologic interpretations and photogrammetric analyses, field and laboratory analyses of soils, and seismic-refraction profiles to characterize the morphology of late Cenozoic lava flows and to measure rates and types of long-term geomorphic processes. Morphologic measurements were made within representative areas on K-Ar–dated flow surfaces. Mesoform parameters—that is, constructional relief, constructional form (small landforms such as pressure ridges developed on the flows during the eruption) frequency, drainage line frequency, percentage of surfaces covered by stone pavements—were measured whenever these

**Additional material for this article may be secured free of charge by requesting Supplementary Data 85-30 from the GSA Documents Secretary.**

Geological Society of America Bulletin, v. 96, p. 1518–1529, 12 figs., 4 tables, December 1985.

turbidite. Turbidites are common on the continental rise below the study area (Piper, 1975; Stow, 1981), although we have insufficient core coverage to demonstrate any specific correlations. Hampton (1972), on theoretical grounds, predicted that some subaqueous debris flows should transform into turbidity currents. Our study area may record a transition from slumping through debris flows to turbidity currents, as he proposed.

### Age and Cause of the Sliding and Debris Flows

Sediment units 1 and 2 overlie the disturbed zones, and unit 1 overlies the steplike slide scarps. Unit 2 was probably genetically related to the sliding and may have accumulated very rapidly. The resedimented shell dated at 12,000 yr B.P. (core 1, unit 3) places a maximum age on the sliding, whereas the faunal change near the base of unit 1 dated between 5000 and 8500 yr B.P. by Hill (1981) provides a minimum age.

Seismic-reflection profiles show that disturbed-sediment zones and sliding of surface sediment are not frequent events within the stratigraphic sequence of the study area. The slide-detachment scarps and the disturbed zones are both surface features, which are usually covered by <2 m of younger sediment that, although found in cores, is generally not detectable on 3.5-kHz profiles. Bedding-plane slides occur over an area of at least 50 × 50 km, in water depths of 800 to 2,500 m, and on gradients as low as 2.5°. Preliminary geotechnical analysis of cores (E. Hivon and K. Moran, 1984, personal commun.) shows that under static conditions the sea-bed sediments are stable on slopes in excess of 15°. This sliding is, therefore, not the result of oversteepening by valley undercutting. The water depth of the slides indicates that they are not triggered by cyclic loading by storm waves on the upper slope. Although Hill and others (1983) suggested that creep may lead to sediment detachment, there is no apparent reason for this process to be restricted in time and space, and evidence for active creep is seen at only one locality (Fig. 5). The sliding, consequently, is most probably seismically triggered. The continental margin off eastern Canada is an area of rare large-magnitude earthquakes (Basham and Adams, 1982). The geographic extent of sediment slides in the Verrill Canyon area is similar to that around the 1929 Grand Banks earthquake epicenter (Piper and others, 1985), suggesting that the two earthquakes that triggered the slides were of similar magnitude.

## CONCLUSIONS

Between 5000 and 12,000 yr B.P., a large earthquake appears to have caused widespread surface sediment failure over an area 50 km by 50 km on the Scotian Slope west of Verrill Canyon. The upper 10–20 m of sediment failed over large areas, leaving steplike escarpments. Much of this sediment formed two acoustically distinct disturbed-sediment zones that thin downslope. Rotational slumping involving little downslope transport was probably the dominant mechanism, although some true debris-flow deposits occur distally. Turbidity currents developed from these debris flows and scoured the lower parts of the debris flows and the sea bed beyond them.

## ACKNOWLEDGMENTS

We thank Keith Manchester, Bill Ryan, Dale Chayes, Kim Kastens, and Suzanne O'Connell for assistance with the Sea MARC I data collection, and Don Bidgood for v-fin sparker profiles. Edna Wilson, Gordon Cameron, and Davis Mosher helped to describe cores. Peta Mudie and Gus Vilks provided biostratigraphic data. Capt. Fred Maugher and the officers and crew of C.S.S. *Hudson* handled Sea MARC in an unusual tow configuration. Roy Sparkes assisted in many parts of the data interpretation. The manuscript was reviewed by P. R. Hill and J.P.M. Syvitski and was greatly improved by two anonymous referees. This work was supported by the Canadian Office of Energy Research and Development.

### REFERENCES CITED

Basham, P. W., and Adams, J., 1982, Earthquake hazards to offshore development on the eastern Canadian continental shelves: Canadian Conference on Marine Geotechnical Engineering, 2nd, Proceedings.
Belderson, R. H., and Kenyon, N. H., 1976, Long-range sonar views of submarine canyons: Marine Geology, v. 22, p. M69–M74.
Bidgood, D.E.T., 1974, A deep-towed sea bottom profiling system: Proceedings of the Oceans 74 Institute of Electrical and Electronic Engineers Conference. Institute of Electrical and Electronic Engineers, New York, v. 2, p. 96–107.
Cook, H. E., Field, M. E., and Gardner, J. V., 1982, Characteristics of sediments on modern and ancient continental slopes, *in* Scholle, P., and Shearing, D., eds., Sandstone depositional environments: American Association of Petroleum Geologists Memoir 31, p. 329–364.
Embley, R. W., 1976, New evidence for the occurrence of debris flow deposits in the deep sea: Geology, v. 4, p. 371–374.
——— 1982, Anatomy of some Atlantic margin sediment slides and some comments on ages and mechanisms, *in* Saxov, S., and Nieuwenhuis, J. K., Marine slides and other mass movements: New York, Plenum Press, p. 189–213.
Farre, J. A., McGregor, B. A., Ryan, W.B.F., and Robb, J. M., 1983, Breaching the shelfbreak: Passage from youthful to mature phase in submarine canyon evolution, *in* Stanley, D. J., and Moore, G. T., eds., The shelfbreak: Society of Economic Paleontologists and Mineralogists Special Publication 33, p. 25–39.
Hampton, M. A., 1972, The role of subaqueous debris flow in generating turbidity currents: Journal of Sedimentary Petrology, v. 42, p. 775–793.
Hill, P. R., 1981, Detailed morphology and late Quaternary sedimentation of the Nova Scotian slope, south of Halifax [Ph.D. thesis]: Halifax, Nova Scotia, Dalhousie University, 331 p.
——— 1983, Morphology of a small area of the Scotian Slope at 63° W: Marine Geology, v. 53, p. 55–76.
——— 1984, Sedimentary facies on the Nova Scotian upper and middle Continental Slope, offshore Eastern Canada: Sedimentology, v. 31, p. 293–309.
——— 1985, Facies and sequence analysis of Nova Scotia Slope muds: Turbidite vs. hemipelagic deposition: Geological Society of London Special Publication 14, p. 311–318.
Hill, P. R., Moran, K. M., and Blasco, S., 1983, Creep deformation of slope sediments in the Canadian Beaufort Sea: Geomarine Letters, v. 2, p. 163–170.
Kastens, K., and Shor, A., 1985, Evolution of a channel meander on the Mississippi Fan: American Association of Petroleum Geologists Bulletin, v. 69, p. 190–202.
Kenyon, N. H., Belderson, R. H., and Stride, A. H., 1978, Channels, canyons and slump folds on the continental slope between southwest Ireland and Spain: Oceanologica Acta, v. 1, p. 369–380.
King, L. H., 1980, Aspects of regional surficial geology related to site investigation requirements, Eastern Canadian Shelf, *in* Ardus, D. A., ed., Proceedings, Offshore Site Investigation: London, Geological Society of London, p. 38–59.
Kosalos, J., and Chayes, D., 1983, A portable system for ocean bottom imaging and charting, *in* OCEANS 83: Third Working Symposium on Oceanographic Data Systems Proceedings, p. 1–8.
LaRochelle, P., Chagnon, J. Y., and Lefebvre, G., 1970, Regional geology and landslides in the marine clay deposits of eastern Canada: Canadian Geotechnical Journal, v. 7, p. 145–156.
Middleton, G. V., and Hampton, M. A., 1976, Subaqueous sediment transport and deposition by sediment gravity flows, *in* Stanley, D. J., and Swift, D.J.P., eds., Marine sediment transport and environmental management: New York, Wiley, p. 197–218.
Nardin, T. R., Hein, F. J., Gorsline, D. S., and Edwards, B. D., 1979, A review of mass movement processes, sediment and acoustic characteristics, and contrasts in slope and base of slope systems versus canyon-fan-basin floor systems, *in* Doyle, L. J., and Pilkey, O. H., eds., Geology of continental slopes: Society of Economic Paleontologists and Mineralogists Special Publication 27, p. 61–73.
Normark, W. R., Piper, D.J.W., and Hess, G. R., 1979, Distributary channels, sand lobes and mesotopography of Navy Submarine Fan, California Borderland: Sedimentology, v. 26, p. 749–774.
Piper, D.J.W., 1975, Late Quaternary deep-water sedimentation off Nova Scotia and the Western Grand Banks: Canadian Society of Petroleum Geologists Memoir, v. 4, p. 195–204.
Piper, D.J.W., and Wilson, E., 1983, Surficial geology of the upper Scotian Slope west of Verrill Canyon: Canada Geological Survey Open-File Report 939.
Piper, D.J.W., Sparkes, R., Farre, J. A., and Shor, A., 1983, Mid-range sidescan and 4.5 kHz sub-bottom profiler survey of mass movement features, Scotian Slope at 61°40′ W.: Canada Geological Survey Open-File Report 938.
Piper, D.J.W., Sparkes, R., Mosher, D. C., Shor, A. N., and Farre, J. A., 1985, Seabed instability near the epicentre of the 1929 Grand Banks earthquake: Canada Geological Survey Open-File Report 1131.
Prior, D. B., and Coleman, J. M., 1982, Active slides and flows in underconsolidated marine sediments on the slopes of the Mississippi Delta, *in* Saxov, S., and Neiuwenhius, J. K., eds., Marine slides and other mass movements: New York, Plenum Press, p. 21–49.
Prior, D. B., Coleman, J. M., and Bornhold, B. D., 1983, Results of a known seafloor instability event: Geomarine Letters, v. 2, p. 117–122.
Ryan, W.B.F., 1982, Imaging of submarine landslides with wide-swath sonar, *in* Saxov, S., and Neiuwenhius, J. K., eds., Marine slides and other mass movements: New York, Plenum Press, p. 175–188.
Stanley, D. J., and Silverberg, N., 1969, Recent slumping on the continental slope off Sable Island Bank, southeast Canada: Earth and Planetary Science Letters, v. 6, p. 123–133.
Stanley, D. J., Swift, D., Silverberg, N., James, N. P., and Sutton, R. G., 1972, Late Quaternary progradation and sand spillover on the outer continental margin off Nova Scotia, southeast Canada: Smithsonian Contributions to Earth Sciences, no. 8, 88 p.
Stow, D.A.V., 1981, Laurentian Fan: Morphology, sediments, processes and growth pattern: American Association of Petroleum Geologists Bulletin, v. 65, p. 375–393.
Swift, S. A., 1985, Late Pleistocene sedimentation on the continental slope and rise off western Nova Scotia: Geological Society of America Bulletin, v. 96, p. 832–841.

MANUSCRIPT RECEIVED BY THE SOCIETY FEBRUARY 17, 1984
REVISED MANUSCRIPT RECEIVED APRIL 24, 1985
MANUSCRIPT ACCEPTED MAY 23, 1985

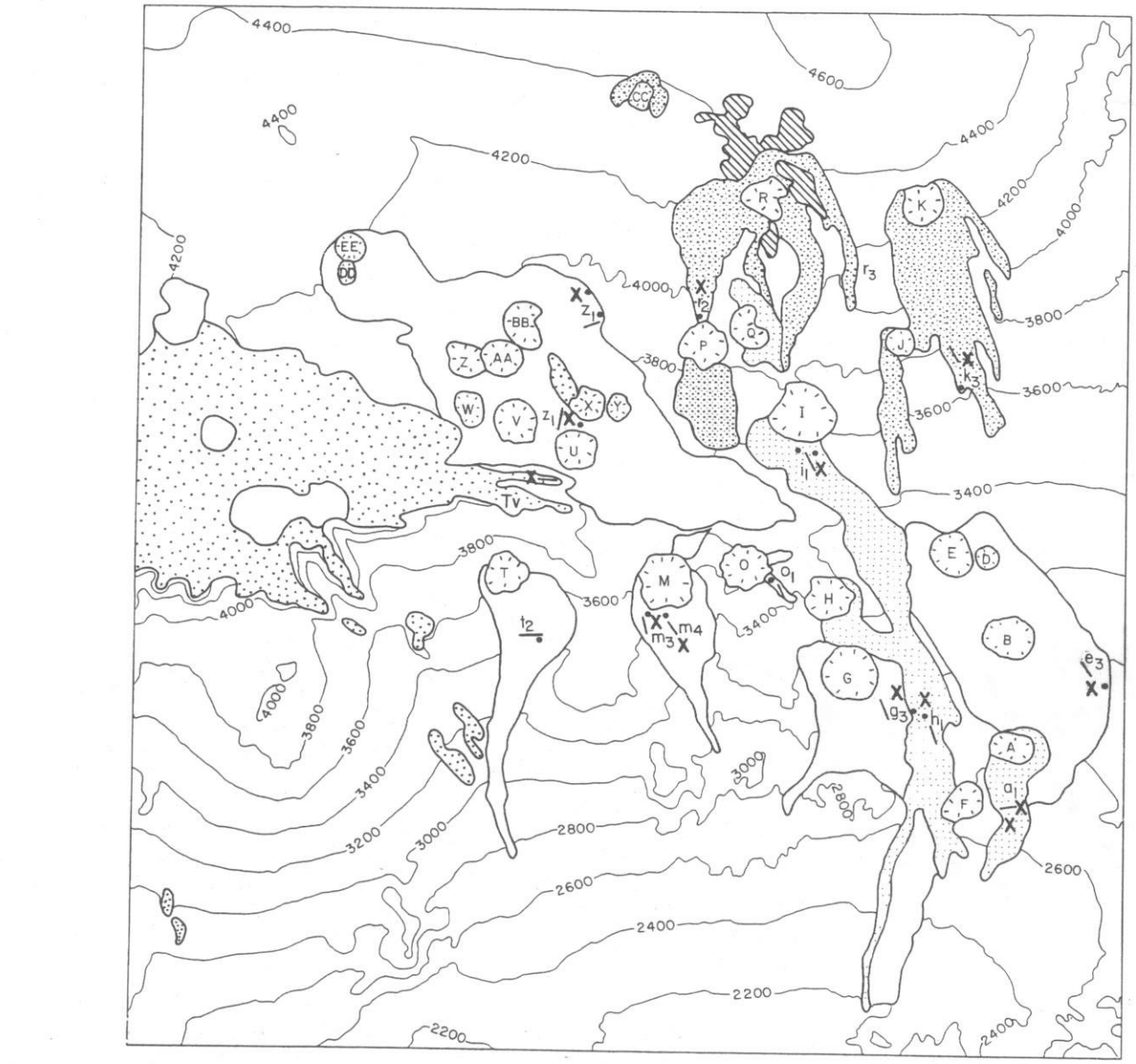


**Figure 1. Generalized map of the Cima volcanic field showing the locations of morphologic transects (—), soil pits (X), and K-Ar samples (.).**

features were encountered along 300- to 1,000-m closed traverses. Microform parameters (that is, clast size, clast relief) were measured every 0.5 to 1.0 m along 50- to 100-m linear transects. Drainage frequencies and densities were measured from 1:20,000 nominal-scale, color, vertical aerial photographs. Field data on bedrock exposure and areal extent of accretionary mantles were supplemented by measurements made with a digital planimeter-Videoplan computer system from the same aerial photographs.

Soil profiles were examined in pits excavated on the most level and stable parts of accretionary mantles on dated lava flows. The soils were described primarily according to the terminology of the *Soil Survey Manual* (Soil Survey Staff, 1951). Samples from each horizon were collected for analysis of soil particle-size distribution.

Seismic-refraction profiles were measured on four flows. Each refraction line consisted of a forward and a reverse end-shot with each shot point located at a distance from the end of the line equal to the geophone

separation distance. P-wave traveltimes were recorded using a 12-geophone line and an EG & G GeoMetric/Nimbus 1210F Signal Enhancement seismograph. Data were analyzed using the standard slope-intercept analysis method. The P-wave traveltimes were plotted against shot-geophone distances, and straight-line segments were fitted to the data to calculate depths to refractors and P-wave velocities of the refracting median.

## GEOLOGIC SETTING AND GEOMETRY OF THE CIMA BASALT FLOWS

The Cima volcanic field contains ~40 basaltic cones and >60 associated lava flows that collectively cover ~150 $km^2$ of pedimented pre-Tertiary crystalline rocks and thick deposits of Tertiary gravels (Fig. 1) (Dohrenwend and others, 1984a). The flows are 100 to 1,700 m wide, 700 to 9,100 m long, and range from rough and essentially unmodified younger flows to smooth, highly modified older flows (Fig. 2). Flows in the Cima volcanic field form a continuum between two distinct morphologic types: (1) elongate flows having low gradients and relatively low original surface relief and (2) approximately equant flows having high gradients and relatively high original surface relief. Elongate flows display many of the surficial flow features that are characteristic of pahoehoe and aa flows formed on moderate gradients such as leveed flow channels, closely spaced pressure ridges, irregular collapse depressions, rafted spines and spires, and lobate to digitate flow margins. Elongate flow thicknesses vary from 2.5 to 4 m except where locally ponded. Flow gradients range from ~3% to 6% with a mean gradient of 4.5% (Dohrenwend and others, 1984a). Morphological measurements and comparisons of flow-surface morphology were limited to the elongate flows, because they show the strongest morphological changes with time, (Fig. 2) and probably they had relatively similar initial flow morphologies.

## GEOMORPHOLOGY OF LATE CENOZOIC VOLCANIC-FLOW SURFACES

### Morphology of Quaternary Flow Surfaces

Surfaces of the basalt flows less than 1.0 m.y. old in the Cima field are composed of constructional bedrock forming topographic highs and accretionary mantles formed in topographic lows. Relative proportions of these two surface types vary with flow age (Table 1; Fig. 2). Accretionary mantles cover 23% to 58% of flow surfaces on flows less than 0.20 m.y. old

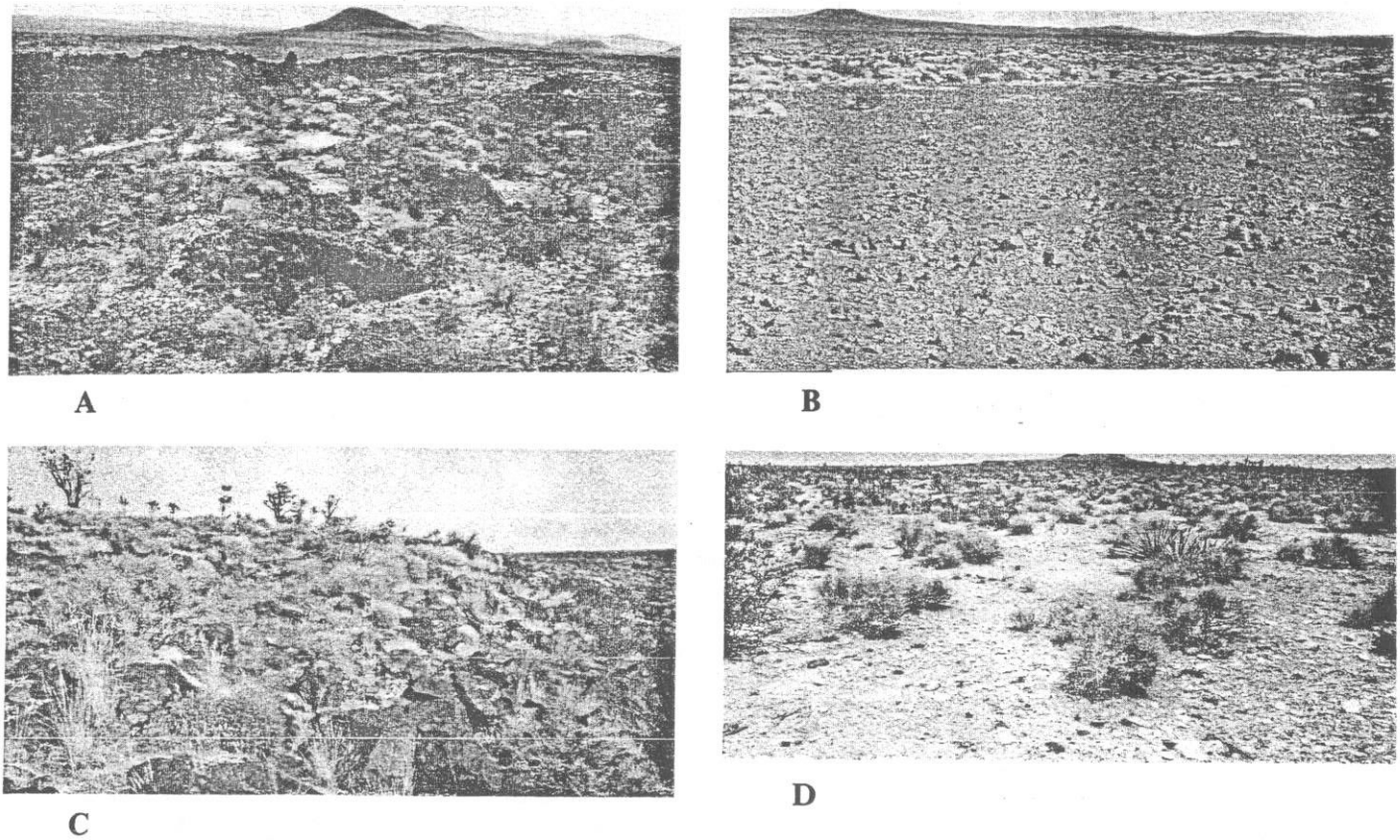


**Figure 2. Comparison of flow-surface morphology for late Cenozoic basaltic flows in Cima volcanic field. A. Center of late Pleistocene $i_1$ flow (0.14 ± 0.04 m.y.) with numerous constructional bedrock forms and topographic flows filled with eolian fine sediments (light areas in center of photo). B. Center of mid-Pleistocene $e_3$ flow (0.56 ± 0.08 m.y.) with few constructional bedrock forms and an extensive stone pavement and underlying accretionary mantle. C. Edge of early Pleistocene $r_3$ flow (0.85 ± 0.05 m.y.), with deep dissection and basaltic bedrock exposed along flow margin (note convex-upward flow-surface profile). D. Center of Pliocene flow with no constructional forms, very low relief, and surface mantle of caliche rubble.**

TABLE 1. MORPHOLOGIC PROPERTIES OF SELECTED BASALT FLOWS, CIMA VOLCANIC FIELD

| Flow designation | Flow age* (m.y.) | Transect lengths (m) | Constructional forms | | | Percent mantle and associated stone pavement on flow |
|---|---|---|---|---|---|---|
| | | | Frequency (no./1,000 m) | Density (no./km$^2$) | Relief (m) | |
| $h_1$ | 0.06 ± 0.03 | 900 | 40 | 649 | 1.1–2.8 | 50 |
| $i_1$ | 0.14 ± 0.04 | 860 | 16 | 419 | 1.0–2.3 | 58 |
| $z_1$ | 0.25 ± 0.05 | 500 | 8 | 86 | 0.5–1.0 | 79 |
| $l_2$ | 0.27 ± 0.07 | 300 | 7 | .. | 0.5–0.6 | 94 |
| $m_3$ | 0.39 ± 0.08 | 500 | 6 | 60 | 0.3–1.0 | 86 |
| $g_3$ | 0.46 ± 0.08 | 650 | 6 | 86 | 0.6–1.1 | 88 |
| $e_3$ | 0.56 ± 0.08 | 600 | 3 | 52 | 0.4–1.2 | 84 |
| $m_4$ | 0.75 ± 0.22 | 330 | 9† | .. | 0.3–0.5 | 84 |
| $k_3$ | 0.99 ± 0.07 | 1,060 | 1 | 8 | 0.0 | 66 |

*Note:* refer to Figure 1 for flow locations.
*Radiometric ages from Dohrenwend and others (1984a); ± values are 2 sigma error ranges.
†This high constructional form frequency is probably due to the steeper slope of flow $m_4$ compared to other flows.

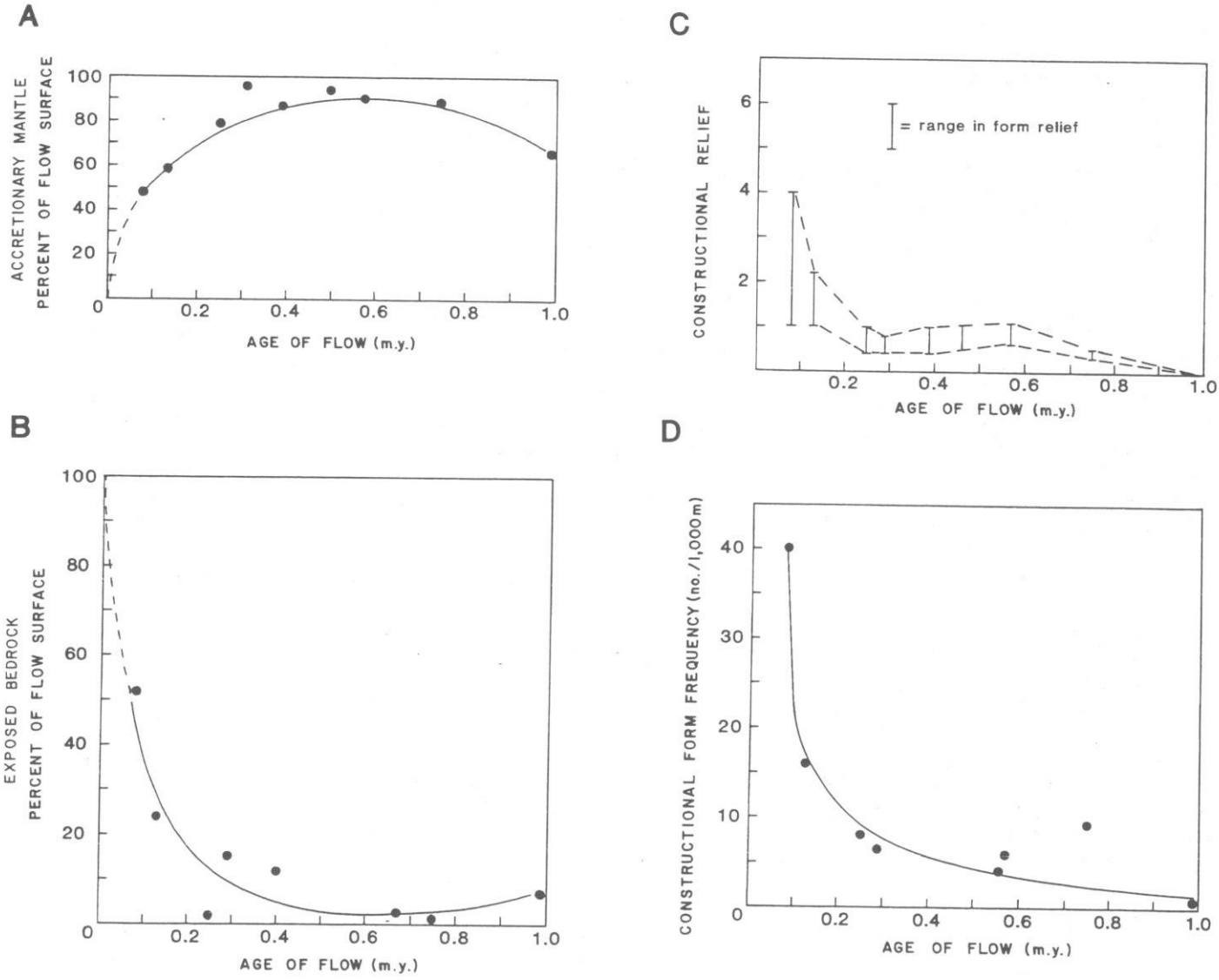


Figure 3. Variation in surface characteristics on selected Quaternary lava flows in the Cima volcanic field. A. Changes in percentage of surfaces covered by accretionary mantles (determined from field transects only). B. Changes in percentage of surfaces with exposed bedrock (determined from photogeologic measurements and independent from data shown in A). C. Changes in relief on constructional forms. D. Changes in frequency of constructional forms. (*Note*: each point represents one dated flow, and lines are visual fits.)

TABLE 2. DRAINAGE NETWORK PROPERTIES OF SELECTED BASALT FLOWS, CIMA VOLCANIC FIELD

| Flow | Age | Drainage frequency (no./1,000 m)* | Drainage frequency (no./km²)† | Drainage density (km/km²)† |
|---|---|---|---|---|
| $h_1$ | 0.06 ± 0.03 | 1 | 8 | 1.1 |
| $i_1$ | 0.14 ± 0.04 | 1 | 3 | 0.6 |
| $z_1$ | 0.25 ± 0.05 | 4 | 23 | 5.2 |
| $t_2$ | 0.27 ± 0.07 | 1 | .. | .. |
| $m_3$ | 0.39 ± 0.08 | .. | 40 | 7.2 |
| $g_3$ | 0.46 ± 0.08 | 3 | 83 | 11.0 |
| $e_3$ | 0.56 ± 0.08 | 5 | 77 | 9.9 |
| $z_3$ | 0.67 ± 0.13 | .. | 71 | 10.6 |
| $r_2$ | 0.70 ± 0.06 | .. | 80 | 11.1 |
| $m_4$ | 0.75 ± 0.22 | 6 | .. | .. |
| $r_3$ | 0.85 ± 0.05 | .. | 100 | 9.5 |
| $k_3$ | 0.99 ± 0.07 | 12 | 123 | 14.9 |

*Note:* see Figure 1 for flow locations.
*Field measurements.
†Photogeologic measurements.

and 80% to 95% of surfaces on 0.25- to 0.75-m.y.-old flows (Fig. 3A).[1] On flows older than 0.75 m.y., commonly only 70% or less of flow surfaces are covered by the accretionary mantles; along flow margins, flow surfaces are being stripped and dissected (Fig. 2C). Re-exposed flow surfaces show little to no original constructional morphology; rather, they are deeply degraded.

Frequency, density, and relief of constructional volcanic landforms developed on flow surfaces also show systematic changes with flow age (Table 1; Figs. 3C, 3D). Decreasing relief, density, and frequency of constructional forms occur on progressively older flows as the areal extent and thickness of the accretionary mantle increase. Variation of relief on flows younger than 0.15 m.y. is >1.0 m, whereas relief typically varies <0.7 m on flows 0.25 m.y. and older. The frequency and density of constructional forms also decrease on older flow surfaces (Table 1; Fig. 3D). The greatest reduction in relief, density, and frequency of constructional forms occurs on flow surfaces between 0.14 and 0.25 m.y.

Drainage development on flow surfaces also shows systematic changes with increasing flow age (Table 2; Fig. 4). Field and aerial photogeologic measurements show drainage frequency increases as flows become progressively older. The relation of field-measured drainage frequency ($D_f$) and flow age (T) is expressed by the equation $D_f = -0.56 + 10.77\ T$ ($r = 0.924$, significant at $\alpha = 0.01$) and indicates that drainage frequency has developed at a nearly constant rate throughout most of the last one million years (Fig. 4a). Drainage density ($D_d$) changes logarithmically with flow age (T) ($D_d = 12.63 + 4.81\ \ln T$ ($r = 0.925$, significant at $\alpha = 0.01$) (Fig. 4b). Values of drainage density for late to mid-Pleistocene flows increase rapidly and are nearly constant for early Pleistocene flows (Fig. 4b).

Factors such as original flow morphology, flow width, subflow paleotopography, and proximity of volcanic vents influence flow-surface morphology and can cause apparent exceptions to the general trends. The relations between landform morphology and flow age are considered general trends; consequently, some flow surfaces in the Cima field deviate significantly from the trends described above (see flow $m_4$ in Table 1).

[1]Radiometric ages used in this paper are from Dohrenwend and others (1984a). In the interests of readability, age ranges are usually given without the customary error estimates. For the exact radiometric ages upon which these approximate age ranges are based, refer to Table 1 of this paper or to Dohrenwend and others (1984a).

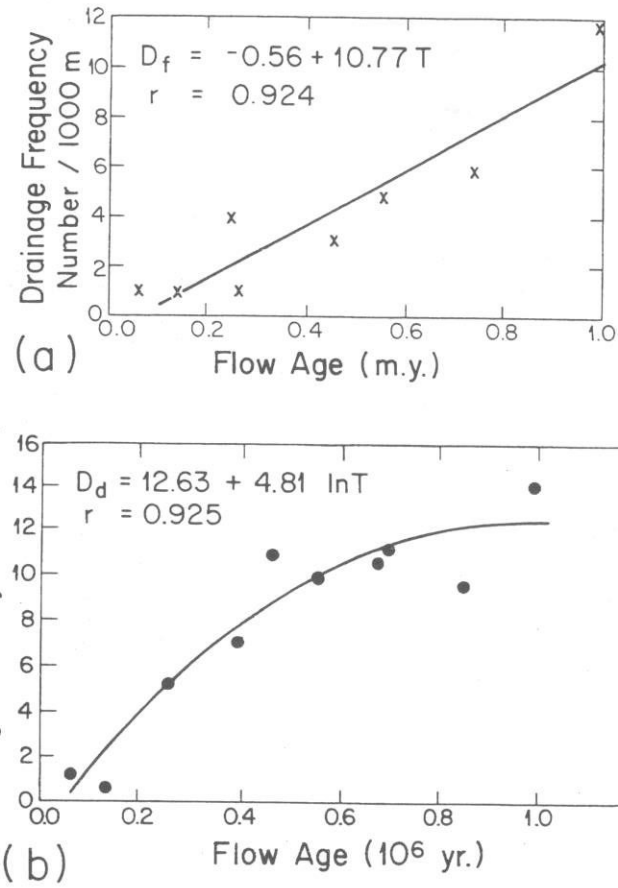


**Figure 4. a. Drainage frequencies ($D_f$) for field measurements made on dated flows of different ages (T); solid line is statistically significant best-fit curve. b. Drainage densities ($D_d$) for dated flows of different ages (T); solid line is statistically significant best-fit curve.**

### Accretionary Mantles Developed on Quaternary Flows

Accretionary mantles developed on basalt flows of the Cima volcanic field, defined primarily on the basis of exposures in 15 soil pits, are composed of 3 general stratigraphic units: (1) a basal rubble zone of angular to subangular basalt clasts derived predominantly from the underlying basalt flow in a matrix of fine sands and silts, (2) an overlying layer composed dominantly of fine sand and silt derived from eolian sources (Figs. 5, 6) and (3) a thin upper layer of basalt clasts forming a stone pavement (Fig. 6). The most laterally continuous exposure of these units can be observed in the lower part of a 25-m long, 2-m deep backhoe trench that has been cut into the surface of flow $r_2$, 0.70 ± 0.06 m.y. (Figs. 1, 7; Table A)[2]. In contrast to most of the flow surfaces in the Cima field, several layers of tephra erupted from a late Pleistocene cone 0.5 km windward of the trench site have buried the accretionary mantle. The uppermost part of the buried accretionary mantle is a stone pavement with varnished clasts similar to subaerially exposed pavements on flow surfaces of comparable age. Underlying the stone pavement is a 0.9-m-thick layer of eolian fine sand and silt in which a well-developed soil has formed

[2]Tables A and B are on file with The Geological Society of America Data Repository. To secure free copies, request Supplementary Data 85-30.

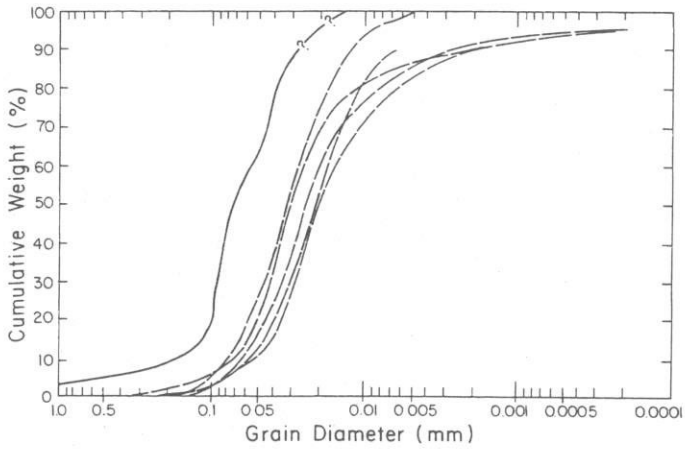


**Figure 5. Comparison of cumulative grain-size distributions of eolian deposits on the Cima lava flows (solid line) and desert dust (dashed lines). Desert-dust grain-size distributions modified from Péwé and others (1981).**

**Figure 6. Upper two layers of the accretionary mantle on a basaltic lava flow in the Cima field: stone pavement veneer over a 1- to 3-m-thick accumulation of eolian fine sand, silt, and clay. Photograph by J. C. Dohrenwend.**

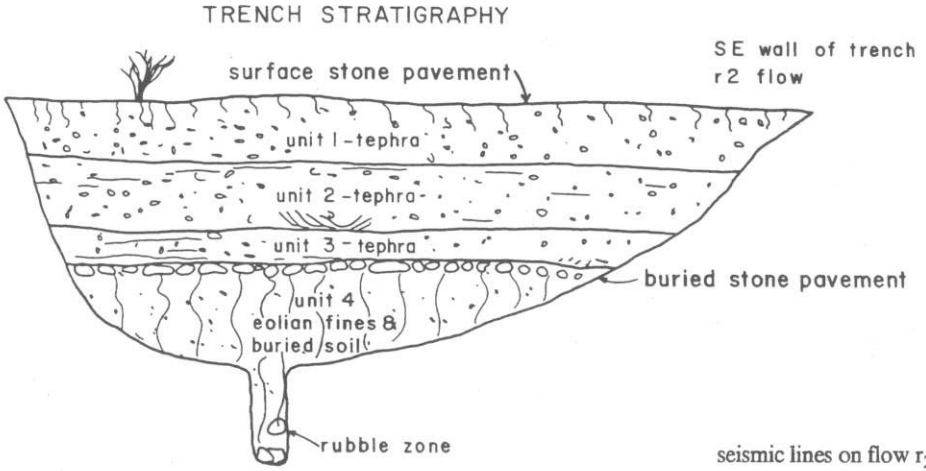


**Figure 7. Stratigraphy of the accretionary mantle exposed in trench on flow $r_2$ (0.70 ± 0.06 m.y.); see Figure 1 for trench location and Table A for stratigraphic descriptions of units.**

(Table A). The only visible contribution of eolian fines to the surface of flow $r_2$ subsequent to its burial are the fine sand and silt that fill pore spaces in the overlying tephras.

Stone pavements composed of clasts of flow rock and vent debris occur on basaltic flows of all ages. They overlie varying thicknesses of relatively clast-free eolian deposits (Figs. 7, 8). Mean clast size on pavements ranges from 3.3 to 10.0 cm on 0.14- to 0.99-m.y. flow surfaces; maximum relief of clasts above pavement surfaces is relatively consistent (14 to 23 cm) for most dated flows. Clast bottoms that project into the underlying soil, moreover, are commonly reddened to hues of 2.5 YR or 5 YR, indicative of some type of chemical alteration during pavement development (Wells and others, 1984a). A stone pavement buried beneath younger mantle deposits on flow $e_3$ (Fig. 1; Table B) shows characteristics similar to the now subaerial stone pavements. This soil-stratigraphic relation suggests that accretionary mantles form episodically with intervening periods of surface stability.

To define the subsurface geometry of the accretionary mantle, seismic-refraction measurements adjacent to the trench on flow $r_2$ were used to calibrate the seismic characteristics of the accretionary mantle and the underlying basalt flow. Velocity-depth profiles for six overlapping seismic lines on flow $r_2$ were drawn parallel to the trench and perpendicular to the flow direction (Fig. 8). Inconsistencies between adjacent lines reflect subsurface heterogeneities and suggest significant variability in the thickness and the degree of compaction of the accretionary mantle as well as substantial irregularity along the mantle–flow rock contact. Comparison of Figures 7 and 8 demonstrates a general agreement between the combined thicknesses of the overlying tephras and the accretionary mantle and the upper velocity layer of the seismic profiles: 2.0 m and 1.0 to 2.5 m, respectively. The upper velocity layer (0.32 to 0.41 km/s) is correlated with the eolian (and pyroclastic) mantle; the middle velocity layer (1.06 to 1.97 km/s) is correlated with the rubble zone; and the deepest velocity layer is correlated with dense, but highly fractured, basaltic flow rock (2.35 to 3.34 km/s). Similar seismic velocities and velocity-layer thicknesses have been determined for three additional lava-flow surfaces in the Cima field (Table 3).

Owing to the inpenetrable nature of the basal rubble zone, only the uppermost few centimetres have been observed in the soil pits. These exposures show basalt clasts in a matrix of fine sediment. Seismic studies on flow $r_2$ support these limited observations. Using the equation of Telford and others (1976) and assuming the middle layer shown in Figure 8 is composed of basalt-clast rubble in a matrix of fine sand and silt, we estimate the range in porosity for the middle layer to be between 12% and 28%.

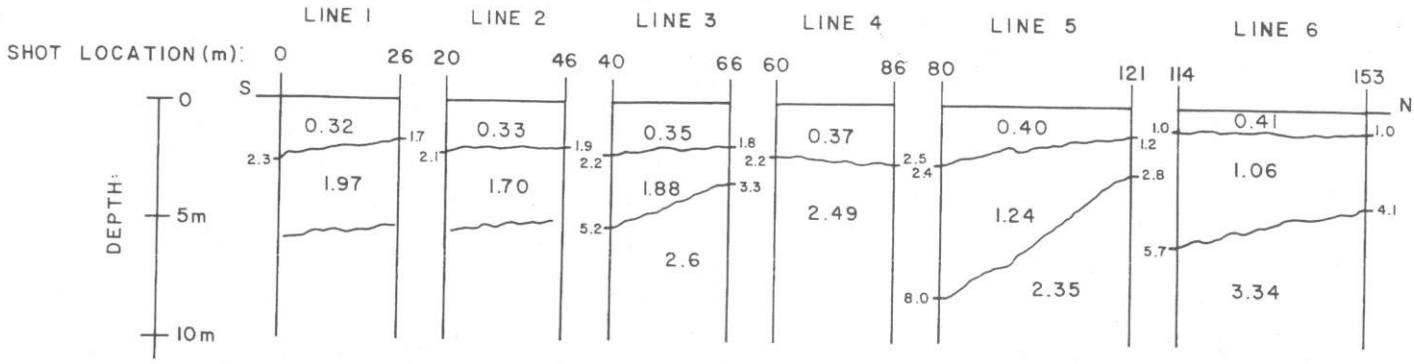


**Figure 8. Seismic P-wave velocity-depth profiles for flow $r_2$. Number within each profile layer is the seismic velocity (km/s) of that layer, and number adjacent to profile segments is depth to interface. Note that the boundaries between profile layers are extrapolated to the end points.**

### Morphology and Mantles of Tertiary Lava-Flow Surfaces

Surfaces of Pliocene flows are flat to gently rolling, are devoid of any constructional bedrock forms, and typically occur tens to hundreds of metres above the surrounding terrain as mesas flanked by thick accumulations of basalt clasts forming colluvial wedges. On aerial photographs, the lighter, moderately uniform Pliocene flow surfaces contrast with the darker, mottled Quaternary flow surfaces. Pliocene flow surfaces are commonly mantled by caliche rubble, presumed to be the result of fragmentation of petrocalcic horizons (Lattman, 1973). Mean clast sizes of the rubble locally range from 17 to 27 cm. Eolian silts in shallow depressions and in the matrix of the caliche rubble and occasional patches of weakly developed stone pavements form a very thin (<1.0 m thick) accretionary mantle on the Pliocene flows. Drainage development is weak and consists of trunk drainages in deep canyons with few shallow tributaries. Trunk drainages commonly head on extremely degraded volcanic vents composed of pyroclastic debris within a framework of dikes and agglutinate layers. Overall, Pliocene flow surfaces form a degradational landscape with thin accretionary mantles and no constructional volcanic forms.

TABLE 3. SEISMIC VELOCITIES AND THICKNESSES OF ACCRETIONARY MANTLES, CIMA VOLCANIC FIELD

| Flow designation | Age (m.y.) | Number of seismic profiles | Mean seismic velocity (km/sec) | Mean thickness (m) | Layer designation |
|---|---|---|---|---|---|
| $g_3$ | 0.46 ± 0.08 | 3 | 0.38 | 2.7 | upper |
| | | 2 | 1.07 | 6.4 | middle |
| | | 2 | 2.31 | .. | lower |
| $e_3$ | 0.56 ± 0.08 | 5 | 0.51 | 2.4 | upper |
| | | 2 | 1.86 | 5.6 | middle |
| | | 2 | 4.26 | .. | lower |
| $r_2$ | 0.70 ± 0.06 | 6 | 0.38 | 1.0 | upper |
| | | 3 | 1.37 | 3.3 | middle |
| | | 3 | 2.80 | .. | lower |
| $r_3$ | 0.85 ± 0.05 | 4 | 0.45 | 1.1 | upper |
| | | 3 | 1.50 | 2.9 | middle |
| | | 3 | 2.66 | .. | lower |

*Note:* see Figure 1 for flow locations.

## SOILS DEVELOPED ON LATE CENOZOIC VOLCANIC FLOWS

Four stages of soil development, defined on the basis of soil morphologic and textural criteria, can be recognized in the accretionary mantles on flows of the Cima volcanic field (McFadden and others, 1984; Dohrenwend and others, 1984a). The stage of soil development is related to a characteristic range of flow ages: (1) stage 1 = 0.01 to 0.15 m.y.; (2) stage 2 = 0.20 to 0.65 m.y.; (3) stage 3 = 0.65 to 1.0 m.y.; and (4) stage 4 = 3.5 m.y. and older.

The initial stage of soil development is characterized by a strongly developed vesicular A horizon, a thin cambic B or oxidized C horizon, and a stage I calcic horizon (calcic horizon terminology after Gile and others, 1966, and Bachman and Machette, 1977). The vesicular A horizon and overlying stone pavement are present at the surface of soils on nearly all basalt flows in the Cima volcanic field. Pedogenic carbonate in stage 1 soils is disseminated in the soil matrix and is segregated as discontinuous coatings on the sides and bottoms of clasts in the soil profile.

Stage 2 soils are substantially more advanced in the degree of soil development and exhibit well-developed argillic B horizons and stage II (locally stage III) calcic horizons. The thicknesses of the argillic horizons range from <0.5 m to <1 m and occasionally extend into the rubble zone underlying fine sand and silt. Argillic horizons are characterized by 7.5YR 5/4 to 4/6 colors and occasionally attain a color of 5YR 5/4. Pedogenic calcium carbonate is segregated mainly as coatings on clasts and as nodules and filaments in the matrix. Carbonate coatings on the bottoms of clasts are thicker (several millimetres) and denser than coatings on clast sides and tops. Depth of pedogenic carbonate accumulation extends into the rubble zone (Tables A and B).

Stage 3 soils are characterized by stage III calcic horizons. Only a few 0.65- to 1.0-m.y.-old flows have soil profiles with well-developed B horizons similar to stage 2 soils. On most of these older flows, argillic B horizons are engulfed by secondary carbonate and are only weakly to moderately developed. Pedogenic carbonate is segregated as nodules or thick pendants associated with basaltic clasts and apparently has displaced clay plasma in the profile.

Stage 4 soils occur on Pliocene flows and are characterized by partly buried blocky fragments of calcium carbonate, or caliche rubble, that are inferred to be the remnants of stage IV to V petrocalcic horizons (McFadden and others, 1984). The caliche-rubble fragments are commonly well laminated and locally they are tens of centimetres thick. Soil profiles are degraded; hence they lack B horizon development, and soil thicknesses probably exceed 0.5 m.

Successively older flows display increasingly advanced morphologic stages of calcic-horizon development that are typical of alluvial desert piedmonts in the southwestern United States (Gile and others, 1981). Maximal development of the B horizon is associated with soils on 0.20- to 0.65-m.y. flows. All flows less than 0.15 m.y. have similar weakly developed soils; all flows greater than 0.65 m.y. are partly to completely engulfed with pedogenic carbonate and show varying amounts of profile

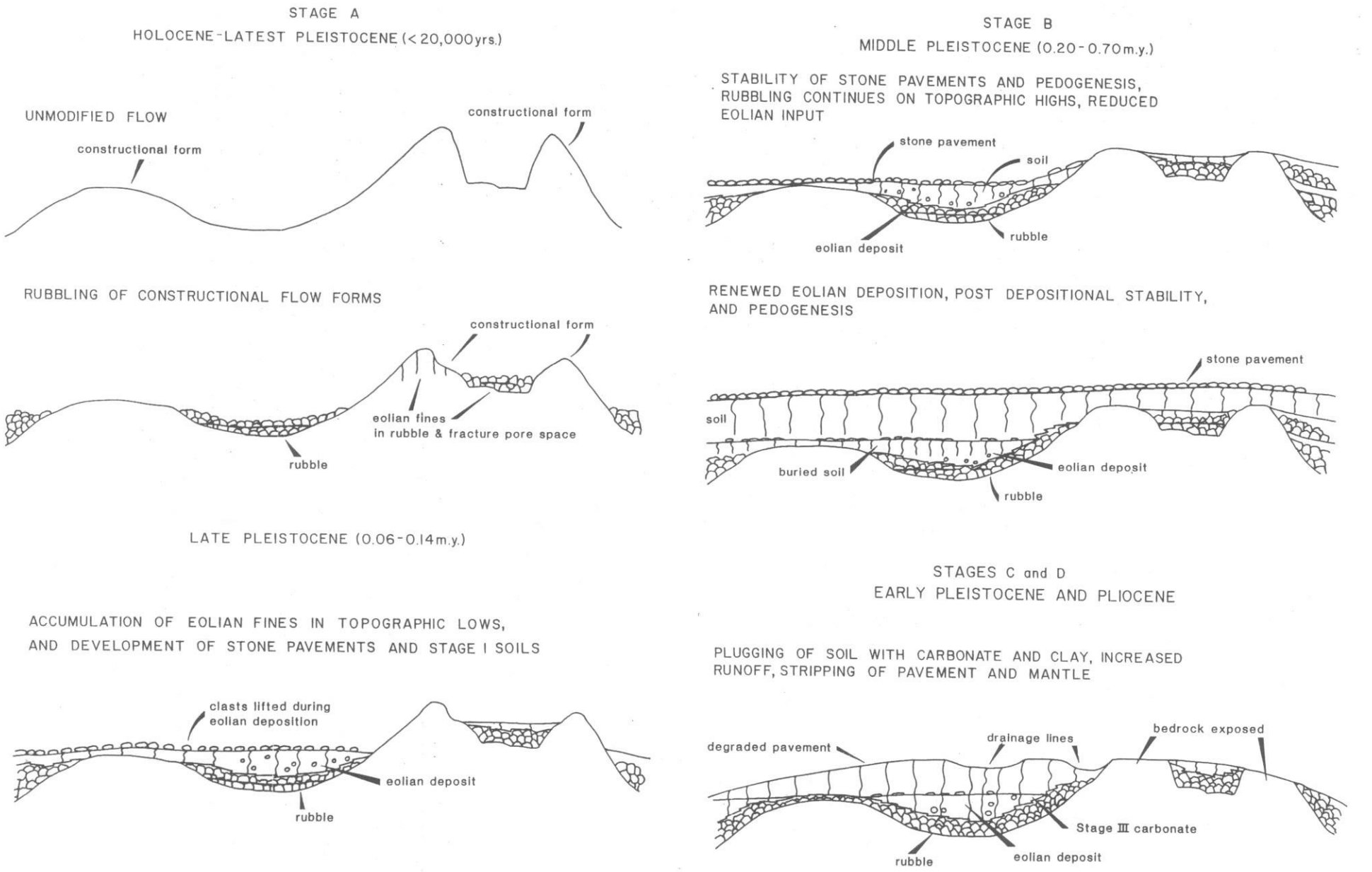


**Figure 9. Schematic topographic and stratigraphic sections of late Cenozoic basaltic lava flows illustrating stages of flow-surface modification. Evolution of basaltic flow surfaces: Stage A: accretionary mantle deformation on flow surfaces by weathering and colluviation of bedrock topographic highs and by eolian deposition in topographic lows. Stage B: flow-surface stability; decreased weathering, colluviation, and eolian deposition; increased soil development; renewed eolian deposition and soil burial; long-term surface stability; development of thick argillic B and carbonate horizons in soils. Stage C: decreased permeability and increased runoff; increased surface erosion, soil stripping, and bedrock exposure. Stage D: petrocalcic fragments (caliche rubble) exposed on deeply dissected flow-capped mesas.**

TABLE 4. STAGES OF LATE CENOZOIC LANDSCAPE EVOLUTION ON BASALT FLOWS IN THE CIMA VOLCANIC FIELD AND THE PROPERTIES ASSOCIATED WITH EACH STAGE

| Stage | Age | Constructional Forms | | Extent of mantle cover† (percentage of flow surface) | Drainage frequency* (no./1,000 m) | Soil profile stage |
|---|---|---|---|---|---|---|
| | | Frequency* (no./1,000 m) | relief (m) | | | |
| A | Holocene to late Pleistocene | >20 | >1.0 | >60 | >1 | 1 |
| B | Middle Pleistocene | 3–8 | 0.3–1.0 | 80–95 | 1–5 | 2 |
| C | Early Pleistocene | >3 | >0.5 | >85 | 6–12 | 3 |
| D | Pliocene | 0 | 0 | .. | <6 | 4 |

*Field measurments. †Photogeologic measurements.

degradation. Occasionally, pedogenic gypsum and silica have also accumulated in these soils (McFadden and others, 1984). In addition, numerous stage 2 and 3 soils in the Cima volcanic field are buried by younger fine sand and silt in which stage 1 soils are developed. For example, a 0.56-m.y. flow is mantled with a stage 1 soil profile overlying a strongly developed stage 2 profile (Table B). The accretionary mantles on flows 0.25 m.y. and older thus are composed of two or more discrete deposits of eolian sediment and represent episodic depositional events separated by intervening periods during which most soil development occurred.

## GEOMORPHIC EVOLUTION OF VOLCANIC FLOW SURFACES

The sequence of dated basalt flows of the Cima volcanic field provides an opportunity to examine landscape evolution by representing time via spatially distinct dated volcanic flows; this is referred to as substituting space for time (Bull, 1975; Schumm, 1977). This approach seems appropriate for analysis of the Cima lava flows, because (1) the petrography and major element chemistry of the flows do not vary significantly, (2) tectonic activity has been minimal, and (3) base level has not changed significantly during the Quaternary (Dohrenwend and others, 1984a, 1984b). Within the framework of past changes in climate, a changing variable through time, the lava-flow surfaces at Cima show systematic changes with increasing age (Figs. 2, 3, 4) and, as described below, are affected by climatic fluctuations.

The evolution of a single flow surface during latest Cenozoic time is characterized by four major stages of landscape evolution and flow-surface modification (Table 4). Each stage represents a period of time when different combinations of surficial processes dominated flow-surface modification (Fig. 9). These stages are useful indicators of approximate age for elongate lava flows, but it is important to note that each stage is not limited to a discrete time interval. Rather, these stages overlap in time, and this overlap is the result of variations in original flow morphology, eolian-sediment flux, local topographic environment, and local base level.

### Evolution of Accretionary Mantles: Role of Weathering and Eolian Deposition

The rubble zone at the base of the accretionary mantle is interpreted to be a combination of original flow-surface rubble (primary rubble) and locally derived basaltic colluvium (secondary rubble). Blocks of flow rock derived from constructional highs are moved into topographic lows by mass wasting and other slope processes. These processes and the infilling of topographic lows with eolian fines reduce the area of exposed bedrock (Figs. 2, 3); consequently, rubble source areas and the potential energy available for rubble movement decrease. Most secondary contributions to the rubble zone thus most likely occur during the early stages of flow-surface modification but prior to significant infilling of topographic lows.

Examinations of bedrock outcrops on younger flow surfaces suggest that mechanical weathering forms most secondary rubble. Field observations and soils data show that significant amounts of eolian fine sand, silt, clay, and soluble salts accumulate in the fractures and vesicles of the basaltic flow rock (Fig. 10). These eolian fines are similar to the fine sand and silt fractions of the accretionary mantles, and high pH values of fines in the mantles indicate high salt concentrations, which are conducive for salt weathering and formation of secondary rubble (Cooke and Warren, 1973). Studies such as those by Lattman (1973) and Peterson (1980) suggest that the probably sources of the salts and eolian materials on the volcanic flows are large playas and distal piedmont areas located upwind from the Cima volcanic field. Episodic eolian events probably have also supplied the large quantities of salt necessary for mechanical weathering of flow rock.

The mantle of fine sand, silt, and clay above the rubble zone also is inferred to be of eolian origin on the basis of grain size and sorting

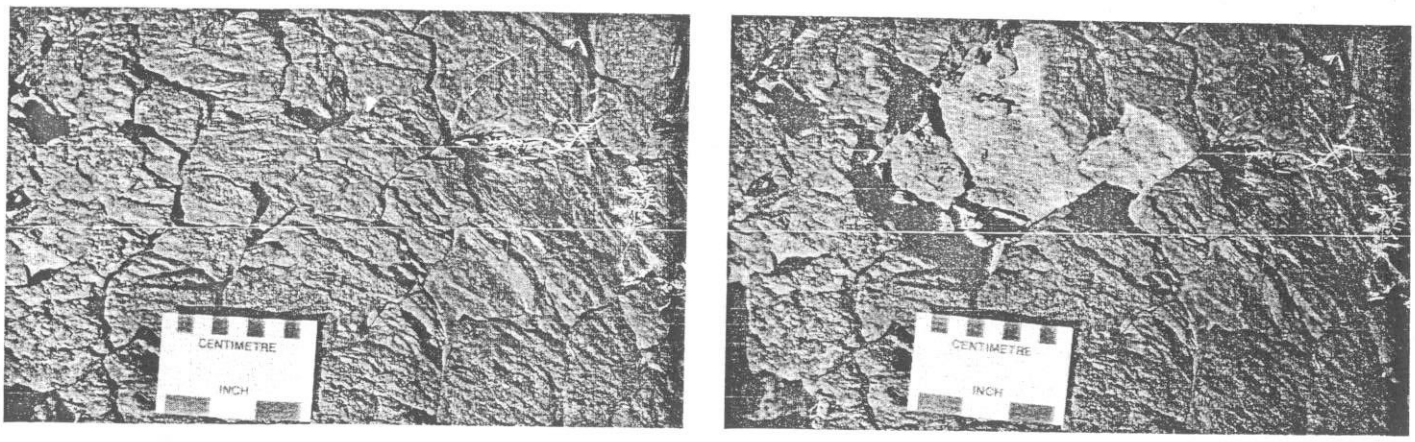


A B

**Figure 10. A. Fractured flow surface on flow $h_1$ (0.06 ± 0.03 m.y.) in the Cima field. B. Same view with surface clasts removed to show silt infilling fractures. Photographs by J. C. Dohrenwend.**

properties (Wells and others, 1984a), as well as the presence of abundant quartz sediment, which indicates sources other than basalt. The majority of mantle sediments are $<0.125$ mm ($3\phi$), are extremely well sorted, and are similar to the grain-size distributions of desert dust (Péwé and others, 1981). Mantle sediments are two times coarser than desert dust, however, which probably reflects proximity to source areas, as well as local saltating loads.

The presence of 1.0- to 2.7-m-thick accretionary mantles with abundant eolian materials on basalt flows suggests that flows are effective eolian traps (Figs. 6, 7, 8). The accumulation of eolian material on flow surfaces is due to (1) high initial surface roughness that causes local reductions in near-surface wind velocities and concomitant deposition of fines and (2) extremely high initial permeability of flows that combines with surface roughness to inhibit surface runoff and fluvial erosion of the trapped silt. Deposition of wind-blown particles at Amboy Crater, California, is greater on lava flows than on adjacent alluvial plains (Greeley and Iversen, 1981). Flow surfaces trap eolian detritus until the surface roughness of the flow is reduced to that of the surrounding terrain (Greeley and Iversen, 1981). Flow surfaces having greater roughness and higher permeability are better eolian traps than smoother flows; therefore, younger, relatively unmodified flows are more efficient traps for eolian fines than older, more degraded flows. Similar observations regarding the influence of surface roughness on eolian accumulations on volcanic bedrock hillslopes have been made by Wells and others (1982) and Ford and others (1982). The presence, however, of eolian deposits with stage 1 soils burying stage 2 and 3 soils, and in some cases stone pavements, demonstrates that profoundly modified flow surfaces with extensively developed accretionary mantles can continue to trap and preserve eolian deposits. Eolian flux rates perhaps were sufficiently high that smoother flow surfaces locally were completely buried.

Rates of eolian deposition can be only approximated from the thickness of eolian deposits on the youngest Cima flow (Fig. 1, flow $a_1$, 16,600 $\pm$ 700 yr B.P.; Dorn, 1984). Eolian deposits in two soil pits (excluding fines filling pore spaces in the rubble zone) are greater than 0.5 m thick, and their average density is 1.65 g/cm$^3$. From field evidence, the lateral contribution of eolian sediments due to water reworking is limited. An average flux rate of 50 g/m$^2$/yr is therefore estimated for the past 16,600 yr. An eolian unit underlying an early Holocene alluvial fan surface adjacent to Silver Lake playa, 20 km northwest of the Cima field, however, is estimated to have been deposited between 10,500 and 9,500 yr B.P. (Wells and others, 1984b). Deposition of most eolian materials on flow $a_1$ also could have occurred during this time period, which would result in an average flux rate of ~800 g/m$^2$/yr, considerably faster than modern flux rates of 40 to 200 g/m$^2$/yr that were measured for desert areas of Arizona, New Mexico, and Israel by Péwé and others (1981), Gile and others (1981), and Yaalon and Ganor (1975), respectively. Given the average thickness of eolian mantles on late to mid-Pleistocene flows (Table 3) and the modern flux rates and derived influx rates, these mantles could have been deposited over periods of $10^3$ to $10^5$ yr.

The occurrence of young stage 1 soils developed in eolian mantles on lava flows less than 0.14 m.y. old and the burial of stage 2 and stage 3 soils on most older lava flows, however, argue against constant flux rates. For example, under constant flux-rate conditions, eolian mantles theoretically could have developed on the 0.14-m.y. flow within 0.04 m.y. of flow emplacement, and pedogenic processes would have produced significantly better-developed soils than those that actually occur on this flow. It thus is more likely that (1) mantles on the younger ($<0.15$ m.y.) Cima flows were formed during the same short-time interval (latest Pleistocene or early Holocene) under extremely high eolian flux rates and (2) the eolian flux rates during the late Pleistocene were so low that significant eolian mantles could not accumulate on flows extruded between 0.015 and 0.15 m.y. ago. Accretionary mantles on flows between 0.25 and 0.65 m.y. typically support stage 2 soils that are buried by stage 1 soils, moreover; this suggests that at least one additional eolian depositional episode has occurred since the formation of the deposits in which stage 2 profiles are developed. This latest eolian episode is inferred to represent the early Holocene event documented near Silver Lake playa (Wells and others, 1984b).

We propose a process-response model based on episodic, rapid influxes of eolian material to explain the formation of eolian mantles. This model emphasizes that the timing of lava-flow eruptions relative to the timing of episodes of high eolian flux is a primary constraint on eolian deposition, soil development, and flow-surface modification in the Cima volcanic field. Short duration, high eolian flux rates might have been caused by intermittent production and limited availability of fines for eolian transport. Playa floors and distal piedmont areas, the most likely primary sources of eolian fines, were episodically exposed during interpluvials of the Quaternary. Eolian sediment would probably have been most available when loose fine sediment was exposed on the dry lake floors and surrounding beaches immediately following the disappearance of the pluvial lakes. Such lacustrine events have been documented under a variety of hydrologic settings in the Mojave Desert (for example, Smith, 1978; Lajoie and Robinson, 1982). During eolian sediment production, the younger Cima flows ($<0.15$ m.y.) would have been mantled by eolian deposits and would have developed similar stage 1 soils during the same time period. Older Cima flows (0.25 to 0.65 m.y.) buried during older eolian events possessed mantles that remained exposed long enough to permit development of stage 2 soils.

### Drainage Network Evolution: Long-Term Hydrologic Adjustments

For the majority of fluvial systems, drainage development over geologic time is inherited from older systems and may reflect conditions the origins of which are difficult to establish (Leopold and others, 1964). Drainage networks developed on volcanic flows, however, originate tens of thousands of years after flow emplacement and are not influenced by previous drainage heritage. Fluvial networks on flow surfaces of successive ages thus provide a time series of drainage development spanning the late Cenozoic on nearly uniform lithology and on surfaces with relatively similar original morphology.

Analyses of drainage network evolution that substitute space for time and describe a sequence of networks on land surfaces of different ages were presented by Glock (1932) and Ruhe (1952). Leopold and others (1964) used drainage patterns on different ages of glacial drift to demonstrate that drainage densities and frequencies increase first rapidly and then more slowly with time. Experimental flume studies (R. S. Parker, unpub. data; Schumm, 1977) documented a similar growth of drainage networks and suggested three stages of growth drainage networks: (1) an initial period of rapid extension, (2) an intermediate period of maximum extension, and (3) a final period of drainage reduction. Glock referred to the three stages as elongation and elaboration (infilling with lower-order streams), maximum extension, and abstraction (loss of drainage lines). In Figure 11, representative drainage networks on Pliocene and Quaternary flows illustrate: (1) initial extension of trunk drainage lines on late Pleistocene flows, (2) network extension by elongation and elaboration on mid- to early Pleistocene flows, and (3) abstraction of drainage lines on Pliocene flows.

Changing drainage densities on progressively older flows are similar to results of experimental studies in flumes and support this sequence of network evolution (Fig. 12). The two growth patterns of drainage networks in flumes are similar to the trend displayed by the flows in the Cima

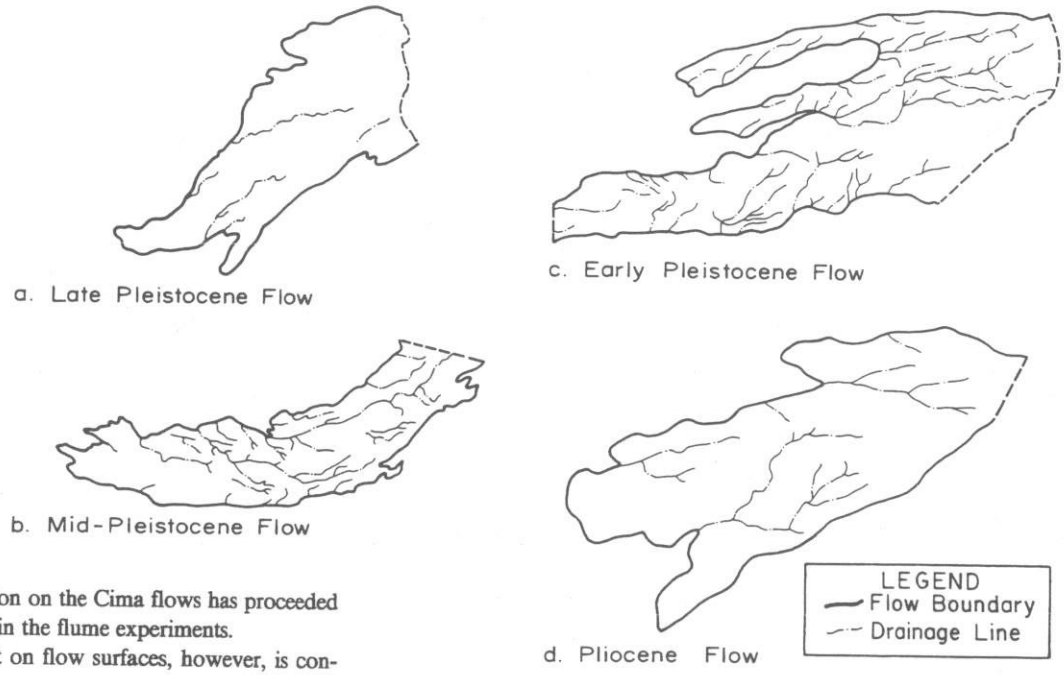


**Figure 11. Drainage networks for selected flows dating from Pliocene to late Pleistocene. Note increasing drainage texture on progressively older flows and decrease in texture on Pliocene flow. Scale approximately equal in all frames, ~1:22,000.**

field, suggesting that drainage evolution on the Cima flows has proceeded in a manner similar to that observed in the flume experiments.

Drainage network development on flow surfaces, however, is controlled initially by the volcanic bedrock (constructional relief and spatial distribution of flow features). Subsequently, drainage networks develop on the accretionary mantles that bury bedrock surfaces. This change influences the relative role of infiltration and runoff on flow surfaces. The primary and secondary rubble and numerous constructional forms on young flow surfaces create a highly permeable surface with large surface roughness, therefore enhancing infiltration. The eolian accretionary mantles and their associated well-developed soils on older flow surfaces decrease the permeability of flow surfaces and reduce the large-scale roughness. Older flows (>0.25 m.y.) thus are characterized by increased runoff and adjust to this hydrologic change by increasing the drainage density and frequency 1 to 2 orders of magnitude (Table 2; Fig. 4).

## DISCUSSION AND CONCLUSIONS

Each major stage in the evolution of flow surfaces (Fig. 9; Table 4) reflects the relative landscape stability of flow surfaces in the Cima volcanic field. Morphologic and pedogenic data indicate that the most stable flow surfaces at Cima occur on flows between 0.2 and 0.7 m.y. (stage B of the landscape-evolution sequence). These stable surfaces are almost completely covered by accretionary mantles and associated stone pavements. The accretionary mantles are characterized by maximum soil-profile development (stage 2 soils), with thick, well-developed argillic B horizons. Flows younger than 0.2 m.y. are undergoing reduction of constructional relief by bedrock weathering, colluviation, and eolian deposition, and they support patchy eolian mantles and weakly developed (stage 1) soils. Flows 0.7 m.y. and older are dominated by surface runoff, fluvial dissection, and partly stripped soils, and they display the maximum drainage-network development (Fig. 4b). Seismic-refraction data show that the thickest accretionary mantles (2.4 to 2.7 m) occur on 0.4- and 0.6-m.y. flows (stage B of landscape-evolution sequence), whereas mantles on older flow surfaces are significantly thinner (1.0 to 1.1 m), suggesting that as much as 1.7 m of eolian fines has been stripped from the mantles of these older flows (Table 2). This decrease in accretionary-mantle thickness is coincident with the time of maximum drainage-network development on the flow surfaces.

The four major stages of flow-surface evolution coincide with the four major stages of soil development on the flow surfaces (Table 4). Changes in the surface morphology of the flows, such as relief reduction

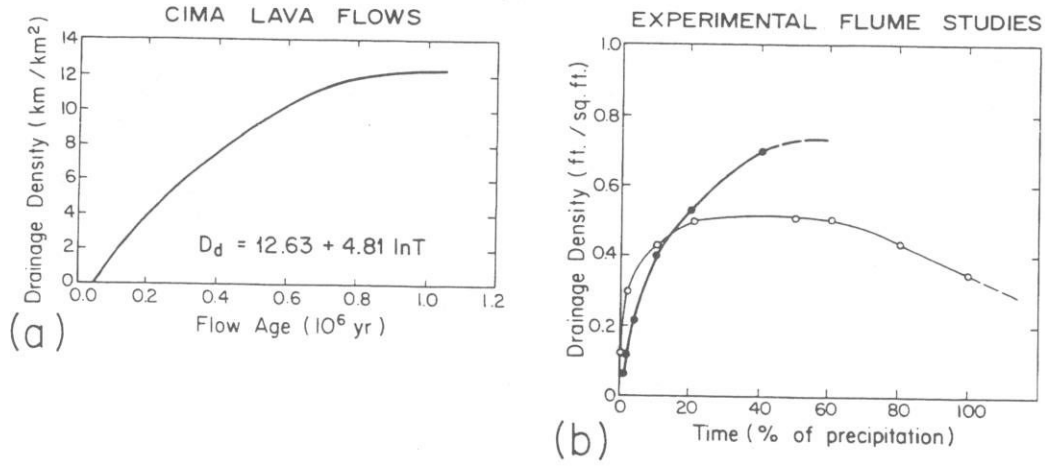


**Figure 12. a. Age-dependent trend shown by best-fit curve in drainage density on basaltic flows using data in Figure 4. b. Drainage density changes during two flume experiments (after R. S. Parker, unpub. data).**

and drainage development, are related to major changes in the soil-profile development. The accretionary nature of the mantles and associated soils on flow surfaces in the Cima volcanic field creates a positive feedback mechanism that affects soil preservation and flow-surface stability. For example, stage 4 petrocalcic horizons are essentially impervious (Cooley and others, 1973); thus, progressive carbonate engulfment of increasingly thick and clay-rich B horizons on relatively stable flow surfaces greatly reduces the infiltration capacities of these surfaces. As a result, B-horizon development decreases with time, and eventually (after ~0.7 m.y.) infiltration capacities are reduced to the point where surface runoff becomes widespread. Fluvial erosion on these older surfaces strips the accretionary mantle and associated soils exposing the underlying plugged carbonate horizons and bedrock. One possible explanation for maximum drainage extension occurring on the early Pleistocene flow surfaces may be related to the impact of soil-profile development and time. Pedogenesis progressively changes the near-surface hydrology (infiltration) which causes regionally stable pervious landscapes to evolve into regionally unstable impervious landscapes on flow surfaces. These attendant changes in geomorphic processes operating on flow surfaces cause a succession of changes in flow-surface stability and morphology.

The stability of flow surfaces not only depends upon evolutionary changes in geomorphic processes but is influenced also by episodic climatically controlled factors such as the influx of eolian fines. Flow-surface stability depends on processes intrinsic to the flow surface, such as weathering and mass wasting of flow-rock outcrops, and the infilling of topographic lows. In addition, stability depends upon the timing of flow emplacement and the duration of subaerial exposure of the flow surface relative to the timing of episodes of high eolian flux. Late Pleistocene flows probably have been exposed to one major eolian depositional episode; middle Pleistocene flows probably have been exposed to at least two such events. The multiple eolian events are at least partly responsible for the strong differences in flow-surface morphology and soil development on flows 0.14 m.y. and younger and flows 0.25 m.y. and older.

## ACKNOWLEDGMENTS

Valuable assistance during field, interpretative, and review phases of this study was generously provided by G. Brem, W. B. Bull, W. Keith, R.S.U. Smith, J. Tinsley, G. Curtis, R. Drake, T. Oberlander, and R. Reynolds. P. Knuepfer, A. Bloom, and an anonymous reviewer provided constructive criticism.

We would like to thank the following people for their assistance in the field and in the laboratory: M. McKittrick, J. Miller, P. Karas, S. Orbock, L. Smith, M. Jackson, M. Boone, B. Elias, J. Ritter, and G. Martinez.

## REFERENCES CITED

Bachman, G. O., and Machette, M. N., 1977, Calcic soils and calcretes of the southwestern United States: U.S. Geological Survey Open-File Report 77794, 163 p.

Bull, W. B., 1975, Allometric change of landforms: Geological Society of America Bulletin, v. 86, p. 1489–98.

Cooke, R. U., and Warren, A., 1973, Geomorphology in deserts: Berkeley and Los Angeles, California, University of California Press, 374 p.

Cooley, R. L., Fiero, G. W., Jr., Lattman, L. H., and Mindling, A. L., 1973, Influence of surface and near-surface caliche distribution on infiltration characteristics and flooding, Las Vegas area, Nevada: Center for Water Resource Research, Desert Research Institute Project Report 21, 41 p.

Dohrenwend, J. C., McFadden, L. D., Turrin, B. D., and Wells, S. G., 1984a, K-Ar dating of the Cima volcanic field, eastern Mojave Desert, California: Late Cenozoic volcanic history and landscape evolution: Geology, v. 12, p. 163–167.

Dohrenwend, J. C., Wells, S. G., Turrin, B. D., and McFadden, L. D., 1984b, Rates and trends of late Cenozoic landscape degradation in the area of the Cima volcanic field, eastern Mojave Desert, California, *in* Dohrenwend, J. C., ed., Surficial geology of the eastern Mojave Desert, California: Geological Society of America 1984 Annual Meeting field trip guidebook, Reno, Nevada, p. 101–115.

Dorn, R. I., 1984, Geomorphological interpretation of rock varnish in the Mojave Desert, *in* Dohrenwend, J. C., ed., Surficial geology of the eastern Mojave Desert, California: Geological Society of America 1984 Annual Meeting Guidebook, Reno, Nevada, p. 150–161.

Ford, R. L., Grimm, J. P., Martinez, G. F., Pickle, J. D., Sares, S. W., Weadock, G. L., and Wells, S. G., 1982, A model of Quaternary desert hillslope evolution: Geological Society of America Abstracts with Programs, v. 14, p. 490.

Gile, L. H., Peterson, F. F., and Grossman, R. B., 1966, Morphological and genetic sequences of carbonate accumulation in desert soils: Soil Science, v. 10, p. 347–360.

Gile, L. H., Hawley, J. W., and Grossman, R. B., 1981, Soils and geomorphology in the Basin and Range areas of southern New Mexico—Guidebook to the Desert Project: New Mexico Bureau of Mines and Mineral Resources Memoir 39, 222 p.

Glock, W. S., 1932, Available relief as a factor of control in the profile of a landform: Journal of Geology, v. 40, p. 74–83.

Greeley, R., and Iversen, J. D., 1981, Eolian processes and features at Amboy Lava field, California: UNESCO Workshop on Physics of Desertification, Proceedings, 23 p.

Lajoie, K., and Robinson, S. W., 1982, Late Quaternary glacio-lacustrine chronology, Mono Basin, California: Geological Society of America Abstracts with Programs, v. 14, p. 179.

Lattman, L. H., 1973, Calcium carbonate cementation of alluvial fans in southern Nevada: Geological Society of America Bulletin, v. 84, p. 3013–3028.

Leopold, L. B., Wolman, M. G., and Miller, J. P., 1964, Fluvial processes in geomorphology: San Francisco, California, W. H. Freeman, 522 p.

McFadden, L. D., Wells, S. G., Dohrenwend, J. C., and Turrin, B. D., 1984, Cumulic soils formed in eolian parent materials on flows of the Cima volcanic field, Mojave Desert, California, *in* Dohrenwend, J. C., ed., Surficial geology of the eastern Mojave Desert, California: Geological Society of America 1984 Annual Meeting field trip guidebook, Reno, Nevada, p. 134–149.

Peterson, F. F., 1980, Holocene desert soil formation under sodium salt influence in a playa-margin environment: Quaternary Research, v. 13, p. 172–186.

Péwé, T. L., Péwé, E. A., Péwé, R. H., Journaux, A., and Slatt, R. M., 1981, Desert dust: Characteristics and rates of deposition in central Arizona: Geological Society of America Special Paper 186, p. 169–190.

Ritter, D. F., 1978, Process geomorphology: Dubuque, Iowa, Wm. C. Brown, 603 p.

Rittmann, A., 1962, Volcanoes and their activity (translation by E. A. Vincent): New York, Wiley-Interscience, 305 p.

Ruhe, R. V., 1952, Topographic discontinuities of the Des Moines lake: American Journal of Science, v. 250, p. 46–56.

Schumm, S. A., 1977, The fluvial system: New York, John Wiley and Sons, 338 p.

Smith, G. I., 1978, Pleistocene geology, Searles valley, California: Guidebook for the 1978 Friends of the Pleistocene-Pacific Coast section meeting, 31 p.

Soil Survey Staff, 1951, Soil Survey Manual: Agricultural Handbook no. 18: Washington, D.C., U.S. Department of Agriculture, U.S. Government Printing Office.

Telford, W. M., Geldart, L. P., Sheriff, R. E., and Keys, D. A., 1976, Applied geophysics: New York, Cambridge University Press, 850 p.

Turrin, B. D., Dohrenwend, J. C., Wells, S. G., and McFadden, L. D., 1984, Geochronology and eruptive history of the Cima volcanic field, eastern Mojave Desert, California, *in* Dohrenwend, J. C., ed., Surficial geology of the eastern Mojave Desert, California: Geological Society of America 1984 Annual Meeting field trip guidebook, Reno, Nevada, p. 88–100.

Wells, S. G., Ford, R. L., Grimm, J. P., Martinez, G. F., Pickle, J. D., Sares, S. W., and Weadock, G. L., 1982, Development of debris mantled hillslopes: An example of feedback mechanisms in desert hillslope processes: American Geomorphological Field Group field trip guidebook, 1982 Conference.

Wells, S. G., Dohrenwend, J. C., McFadden, L. D., Turrin, B. D., and Mahrer, K. D., 1984a, Types and rates of late Cenozoic geomorphic processes on lava flows of the Cima volcanic field, eastern Mojave Desert, California, *in* Dohrenwend, J. C., ed., Surficial geology of the eastern Mojave Desert, California: Geological Society of America 1984 Annual Meeting field trip guidebook, Reno, Nevada, p. 116–133.

Wells, S. G., McFadden, L. D., Dohrenwend, J. C., Bullard, T. F., Feilberg, B. F., Ford, R. L., Grimm, J. P., Miller, J. R., Orbock, S. M., and Pickle, J. D., 1984b, Late Quaternary geomorphic history of the Silver Lake area: An example of the influence of climatic changes on desert piedmont evolution in the eastern Mojave Desert of California, *in* Dohrenwend, J. C., ed., Surficial geology of the eastern Mojave Desert, California: Geological Society of America 1984 Annual Meeting field trip guidebook, Reno, Nevada, p. 69–87.

Wood, C. A., 1980, Morphometric evolution of cinder cones: Journal of Volcanology and Geothermal Research, v. 7, p. 387–413.

Yaalon, D. H., and Ganor, E., 1975, Rates of aeolian dust accretion in the Mediterranean and desert fringe environments of Israel: Congress International de Sedimentologie, 9th, Nice, France, p. 169–174.

MANUSCRIPT RECEIVED BY THE SOCIETY DECEMBER 7, 1984
REVISED MANUSCRIPT RECEIVED JUNE 17, 1985
MANUSCRIPT ACCEPTED JUNE 18, 1985

Printed in U.S.A.

# Eocene amber from the Pacific Coast of North America

GEORGE E. MUSTOE *Geology Department, Western Washington University, Bellingham, Washington 98225*

## ABSTRACT

**Fossil plant resins are common in Late Cretaceous rocks of North America and in Oligocene and younger sediments of equatorial and Southern Hemisphere locations. The scarcity of amber in early Tertiary rocks, however, poses puzzling geological questions. Detailed examination of mid-Eocene amber-bearing sediments from Coalmont, British Columbia, and Seattle, Washington, indicates that resins were produced by taxodiaceous conifers, with *Metasequoia occidentalis* being the most likely source. Laboratory heating experiments and paleotemperature analysis of these sediments based on coal rank and vitrinite reflectance suggest that burial temperatures may significantly affect infrared spectra of amber, a phenomenon not previously recognized by researchers who have long used spectral characteristics to speculate on the botanical origin of fossil resins.**

**The occurrence of amber in mid-Eocene rocks of the Pacific Northwest, Arkansas, and southern California suggests that resin production ended as the climate of North America cooled during the mid-Tertiary and that late Tertiary amber was produced by flowering tropical plants not present in the Eocene forests. This evolutionary record appears somewhat different from that of Western Europe, where progressive southward migration of coniferous amber forests occurred during mid-Tertiary time.**

## INTRODUCTION

Resinous substances have been reported from rocks as old as Carboniferous (Langenheim, 1969), but not until the Late Cretaceous did amber-producing plants flourish. Cretaceous amber is best known from localities in North America, ranging from Greenland and Arctic Alaska to central Canada, the Atlantic Coastal Plain, and various mid-continent locations (Langenheim & Beck, 1968; McAlpine and Martin, 1969; Broughton, 1974). Although many of these deposits consist of amber that was transported by moving water from the original source area, quantities of fossil resin may be quite large; nearly 1,000 kg of amber was collected from the beaches of Cedar Lake, Manitoba, between 1895 and 1937. More commonly, amber occurs as scattered nodules in coal seams or silty sediment. The latter mode of occurrence reflects the very low specific gravity of plant resins, which causes even large lumps to remain in transit until they reach very calm depositional environments.

The botanical origin of these relatively old resins is not well understood. For many years, scientists accepted the views put forth in the late 19th century that amber from Europe was produced by a single species of pine, *Pinus succinifera,* which secreted vast quantities of resin after forests of the Baltic area became infected with disease (Conwentz, 1890, 1896). Later workers suggested that resin secretion represented metabolic leftovers from primitive trees that had not yet developed efficient biochemical pathways. In recent years, the notion of a single species of "amber pine" has been discarded, as has the concept that amber production resulted from disease. Indeed, modern resin-secreting plants typically show the greatest production coming from the healthiest trees (Langenheim, 1969). The prevailing contemporary view is that resin secretion provides an important mechanism for sealing bark wounds and inhibiting attack by insects and herbivores. As these forms of environmental stress are most intense in tropical areas, amber production is most likely to occur in regions having warm, humid climates.

The accumulation of data from North American Cretaceous amber deposits suggests that the probable sources were conifers belonging to the Araucariaceae and Taxodiaceae. The Pinaceae may have been resin contributors in some locations (Langenheim, 1969). The Araucariaceae have been considered because these primitive trees were important elements of Mesozoic forests and because the surviving *Agathis* genus is an important modern source of copal resin in New Zealand and the South Pacific. By the Late Cretaceous, however, members of this group were less abundant in North America than were the Taxodiaceae, which include various members of the redwood and cypress families.

Although millions of kilograms of Eocene amber have been gathered from the Baltic Coast of Denmark and Russia, early Tertiary amber is conspicuously scarce in North America. Despite the great abundance of European amber, its origin is not well understood because the deposits are so difficult to interpret. Eocene amber nodules are found washed up on the modern coast, in Pleistocene glacial sediments, and in Oligocene beach sands. These modes of occurrence eliminate the possibility of examining associated plant fossils or stratigraphic evidence, and the only avenue of study comes from the presence of insects, pollen, and fragments of plant tissue preserved as inclusions within the resin. Results of many decades of Baltic amber research were compiled by Larsson (1978).

Although no amber younger than mid-Eocene has been described from North America, abundant amber occurs in Oligocene-Miocene sediments of Central America. Oligocene beds of the Dominican Republic at present constitute the world's largest source of gem-quality amber, with a production record that dates back many centuries; local residents presented Columbus with a necklace of amber beads to welcome his arrival in the New World. Other amber deposits occur in Mexico, Haiti, Colombia, Chile, and Ecuador (Langenheim, 1969). Late Tertiary amber from equatorial latitudes is strikingly different in botanical origin from older amber. These young resins come from flowering plants rather than conifers, and the deposits commonly occur in regions where resin-producing plants still survive.

The existence of two fundamentally different categories of amber widely separated in age reflects a puzzling evolutionary record for the plant kingdom, because the tendency to produce copious quantities of resin has developed in several unrelated groups of plants. Although amber research historically has been directed at deposits that contain great amounts of resin, from an evolutionary viewpoint the most significant sites for study are deposits that formed during periods when the early coniferous amber forests were dying out and later when new resin-producing plant communities appeared. Ideally, these sediments should contain plant remains and

Geological Society of America Bulletin, v. 96, p. 1530–1536, 5 figs., December 1985.